A Novel Reversible Data-Hiding Method Using Adaptive Rhombus Prediction and Pixel Selection

Thai-Son Nguyen

(Corresponding author: Thai-Son Nguyen)

School of Engineering and Technology, TraVinh University, Vietnam

(Email: corresponding_thaison@tvu.edu.vn)

(Received July 22, 2020; Revised and Accepted Dec. 19, 2020; First Online June 7, 2021)

Abstract

The reversible data hiding (RDH) technique is used to conceal secret data within images such that the original image can be fully recovered upon the extraction of hidden data. Such a technique has attracted much interest from researchers in different fields. In this article, to improve embedding capacity further while maintaining minimum distortion of stego images, a novel reversible data-hiding algorithm is proposed by using the combination of adaptive rhombus prediction and pixel selection. Furthermore, to preserve the image quality well and increase the embedding capacity significantly, the proposed scheme has carefully determined a suitable pixel set and image region for embedding data. The experimental result shows that our method brings better performance than some previous schemes in virtual image quality and embedding capacity.

Keywords: Histogram Shifting; Multiple-Layer Embedding; RDH; Reversibility; Rhombus Prediction

1 Introduction

Reversible data hiding (RDH) is an algorithm that aims to extract embedded secret data exactly and to reconstruct the cover image to its original version without any distortion. Due to these properties, several RDH techniques have been proposed in various fields, such as video error-concealment coding, the military, and medical images [2, 9, 15, 22, 23]. In general, the performance of the RDH technique is evaluated based on the behavior of embedding capacity (EC) and virtual image quality. For a given EC, embedding distortion is maintained as small as possible to achieve good image quality of stego images.

In the last few decades, many RDH schemes that have been proposed can be divided into four types: lossless compression [1, 3, 4, 10, 26], difference expansion (DE) [6, 8, 12, 19, 20, 27, 28], histogram shifting (HS) [5, 7, 11, 13, 14, 16, 18, 21, 25], and integer transform [17, 24]. Among these RDH schemes, HS-based RDH algorithms have attracted much attention of researchers due to good virtual image quality and sufficient EC. The HS-based RDH method was first introduced by Ni *et al.* [16]. In this scheme, Ni et al generated a histogram of the cover image, then they selected peak points and zero points to conceal the secret data. In their scheme, each pixel is altered by no more than one value. Therefore, Ni *et al.*'s scheme achieved a high quality of stego-images; however, its EC is not satisfied when the average EC is always smaller than 7,000 bits. To improve EC further, Hong *et al.* [7] used prediction errors for hiding secret data. In the scheme [7], the high redundancy of pixels is exploited for containing the secret bits. Consequently, their performance is superior to those of DE-based and previous HS-based schemes [16, 19, 20].

In [18], Sachnev *et al.* used rhombus prediction to classify image pixels into two sets – Dot and Cross sets – for HS-based RDH scheme. Their scheme obtained high EC while guaranteeing good image quality. A similar scheme was introduced in [24] with optimal side information selection. Later, a new RDH algorithm, based on the interpolation mechanism, is proposed by Luo *et al.* [14]. In this scheme, interpolation errors are calculated as the difference between the pixel value and the corresponding interpolation value. Then, these difference values are used for hiding the secret message. To guarantee high image quality, in [14], all cover pixels are only altered slightly in the embedding steps; however, the image is distorted significantly when the large EC is embedded. To increase EC while guaranteeing good image quality, in [11], Li et al designed two HS-based schemes by exploiting a nine-dimensional histogram. In their scheme, suitable pixels are selected carefully. Then, two functions, shifting and embedding, are used to generate the room for containing the secret bits. Li *et al.*'s performance was superior to those of previous RDH schemes [11, 12, 14, 18]. Recently, Wang *et al.* [25] proposed a new multiple HS-based RDH technique by employing a genetic algorithm (GA). To maintain reversibility, Wang *et al.* utilized prediction

errors of each pixel to embed secret bit. However, it also causes significant distortion on stego images, if the large EC is embedded.

In this article, a new HS-based RDH method is proposed by combining adaptive rhombus prediction and pixel selection. Inspired by pixel selection techniques proposed in previous schemes [11, 14, 18], for each pixel in this scheme, the local variance value is computed to determine whether it is suitable to embed the secret bit or not. To compute the prediction errors, in the proposed method, an adaptive rhombus prediction algorithm is applied. In addition, to keep the embedding distortion small and the EC high, the optimal information is selected and used during the embedding process. Experimental results demonstrate that the proposed method generates better performance than some previous schemes in terms of EC and image quality.

The remainder of this paper is structured as follows. The brief of Li *et al.*'s method [11] is reviewed in Section 2. Then, Section 3 gives the detail of the proposed method. In Section 4, our proposed method' performance is analyzed in compared with some existing schemes. Eventually, conclusion is provided in Section 5.

2 Related Work

In 2013, Li *et al.* [11] explored a nine-dimensional histogram for hiding the secret message. Take for example, the image block Z sized of 3×3 as shown in Figure 1.

For the first pixel Z_1, the two neighboring pixels Z_2 and Z_4 are used to predict its value by using Equation (1):

$$Z_i' = \left\{ \begin{array}{l} k, \text{ if } Z_1 \geq k \\ l-1, \text{ if } Z_1 < l \end{array} \right\} \quad (1)$$

where $k = max(Z_2, Z_4)$, $l = min(Z_2, Z_4)$, and $k \geq l$.

For embedding the secret data, the local complexity $Com(Z)$ of Z is calculated as Equation (2):

$$Com(Z) = max(Z_2, Z_3, ..., Z_9) - min(Z_2, Z_3, ..., Z_9). \quad (2)$$

After obtaining the local complexity of Z, this local complexity value is used to select the embeddable blocks. To embed a bit b into the block, the $Embed()$ function is used as defined in Equation (3):

$$Embed_b(Z) = \left\{ \begin{array}{ll} (Z_1 + b, Z_2, Z_3, ..., Z_9), & \text{if } Z_1 - k = 0, Com(Z) < T \\ (Z_1 - b, Z_2, Z_3, ..., Z_9), & \text{if } Z_1 - l = -1, Com(Z) < T \\ (Z_1 + 1, Z_2, Z_3, ..., Z_9), & \text{if } Z_1 > k, Com(Z) < T \\ (Z_1 - 1, Z_2, Z_3, ..., Z_9), & \text{if } Z_1 > l-1, Com(Z) < T \\ Z & \text{otherwise} \end{array} \right\} \quad (3)$$

Z_1	Z_2	Z_3
Z_4	Z_5	Z_6
Z_7	Z_8	Z_9

Figure 1: Image block sized of 3×3

where T is the smallest positive integer threshold that is a selected to make sure all of the secret bits to be embedded. Notice that this scheme [11] used the local complexity estimator for selecting embeddable areas in the cover image to achieve a more concentrated histogram. With the local complexity estimator, only blocks with the value of local complexity (smaller than T) will be used to contain the secret bits; however, only the pixel Z_1 of each block sized of 3×3 is used to contain one secret bit, resulting in a limited amount of embedding spaces. Therefore, this scheme is not favorable to hide a large amount of secret data. Obviously, there is a high correlation of the pixels in natural images; therefore, the HS-based RDH schemes seek to achieve high EC and to preserve high-quality stego images; however, these existing schemes are still limited in their performance when the average image quality is smaller than 59 dB for embedding 10,000 secret bits. To overcome these shortcomings, a new RDH scheme is proposed by using a combination of adaptive rhombus prediction and pixel selection, and the detail of which is presented in the next section.

3 Proposed Method

In this section, a novel RDH method is introduced. The flowchart presenting this method is present in Figure 2. The embedding process is briefly described as follows. First, the cover image is separated into two sub-images, *i.e.* A and B. After that, in the sub-image A, all of the pixels is evaluated to classify into two sets, Cross and Dot sets, as can be seen in Figure 3. Then, each set is divided into two parts, *i.e.*, Part 1 and Part 2, consisting of smooth and complex pixels, respectively. To hide the secret data into the Cross set or Dot set, the prediction error histogram of Part 1 is generated. According to the size of the embedded secret data, we optimally select the pair of peak and zero points. Finally, the secret bit is hidden by shifting the prediction error histogram of Part 1. It is noted that pixels in Part 1 are modified by no more than one value, and the Dot set is applied for predicting

pixels of the Cross set, and vice versa. By so doing, the cover image can be prevented from significant embedding distortion. The proposed method can be divided into two subsections, *i.e.* embedding algorithm and extracting algorithm.

3.1 Embedding Algorithm

Assuming that the cover image I with a size of $W \times H$, the secret data $S = s_1, s_2, \ldots s_L$, where $s_i = \{0, 1\}$, and L is the length of S. For embedding data, the image I is divided into sub-image A and sub-image B, as shown in Figure 3. Then, the proposed embedding algorithm is presented as followings.

Step 1 (Pixel partition): Partition the sub-image A into two sets, *i.e.*, Cross (X) and Dot (O) sets, (see Figure 3(a)). After that, the LSBs of pixels in sub-image B is recorded into the bit stream LSB_B. Then, the secret data S is generated by concatenating the bit stream LSB_B into the secret message M.

Step 2 (Pixel selection): To avoid the complexity region, the smooth pixels are selected and used for RDH to decrease embedding distortion as much as possible. The local complexity of each pixel P_X in the Cross set is calculated by using its local-variance (LV) value, defined in Equation (4). Then, the threshold TH is used to determine whether the smooth pixels or not. Equation:

$$LV_P X = dv + dh. \tag{4}$$

where $dh = |P_O^1 - P_O^3|$ is the horizontal variance, $dv = |P_O^2 - P_O^4|$ is the vertical variance, and P_O^i is four adjacent Dot pixels of P_X (see Figure 3(b)). According to the values of the local variance and the selected threshold TH, the pixel P_X is then classified into Part 1 or Part 2 as follows:

- Part 1 (smooth pixels): $P_X \in X : LV_X < TH$.
- Part 2 (complex pixels): $P_X \in X : LV_X \geq TH$.

Step 3 (Computation of prediction errors): For each pixel of Part 1 in the Cross set, according to the values of dv and dh, four adjacent Dot pixels are adaptively used to predict the value of P_X as follows.

$$P'_X = \left\{ \begin{array}{ll} round(\frac{P_O^1 + P_O^3}{2}), & \text{if } dv > dh \\ round(\frac{P_O^2 + P_O^4}{2}), & \text{if } dv \leq dh. \end{array} \right\} \tag{5}$$

Then, calculate the corresponding prediction error EX by Equation (6).

$$E_X = P_X + P'_X. \tag{6}$$

Step 4 (Determination of optimal pair of peak and zero points): As can be seen in existing HS-based RDH techniques, the peak point and the zero point are determined in the prediction error histogram for embedding data. Thus, the embedding capacity C is considered as the frequency of the peak point: $C = F(Peak)$, where $F(.)$ is the frequency function of the histogram. Different from existing HS-base techniques, after obtaining all prediction errors E_X of Part 1 in the Cross set, the proposed method optimally selects pair of peak and zero points in the histogram of E_X for embedding the secret data S as following.

- From the value of 0, scan negative and positive axes of the histogram, to find the first two matched zero points Z_l and Z_r, as shown in Figure 4(a).
- From the point Z_l toward the value of 0, search for a suitable peak point P_l, such that the constraint, $F(P_l) \geq L$, is satisfied.
- Similarly, from the point Z_r toward the value of 0, search for a suitable point P_r, such that the constraint, $F(P_r) \geq L$, is satisfied.
- Among two candidate pairs of peak and zero points, *i.e.*, (P_l, Z_l) and (P_r, Z_r), the optimal one, denoted as (P^*, Z^*), is selected with the smaller shifting distortion.

Step 5 (Embedding process and generation of the stego image): After determining the optimal pair (P^*, Z^*), for hiding the secret data S, all bins between P^* and Z^* are shifted to the Z^* direction to generate room bin near the peak point P^*. Assume that $P^* < Z^*$. Then, each prediction error E_X is processed by either shifting its value if $E_X \in (P^*, Z^*)$ or embedding one secret bit s_i, if $E_X = P^*$, which is defined in Equation (7).

$$E'_X = \left\{ \begin{array}{ll} E_X + 1, & \text{if } E_X \in (P^*, Z^*) \\ E_X + s_i, & \text{if } E_X = P^*. \\ E_X, & \text{otherwise} \end{array} \right\} \tag{7}$$

After that, the stego pixels of Part 1 in the Cross set are computed by using Equation (8).

$$P''_X = P'_X + E'_X. \tag{8}$$

According to the values of stego pixels P''_X in the Cross set, the same steps are used to embed the secret data into pixels of the Dot set to generate stego pixels P''_O. Finally, P''_X and P''_O are combined to generate the stego image.

Instead of directly using the pair of peak and zero points as was done in the existing HS-based techniques, two candidate pairs of peak and zero points are determined, and the optimal one is used to hide secret data. Here, for single-layer embedding, assume that $F(P_l) \geq L$ and $F(P_r) \geq L$; however, if the length of the secret data $L > F(P_l)$ and $L > F(P_r)$, multi-layer embedding with

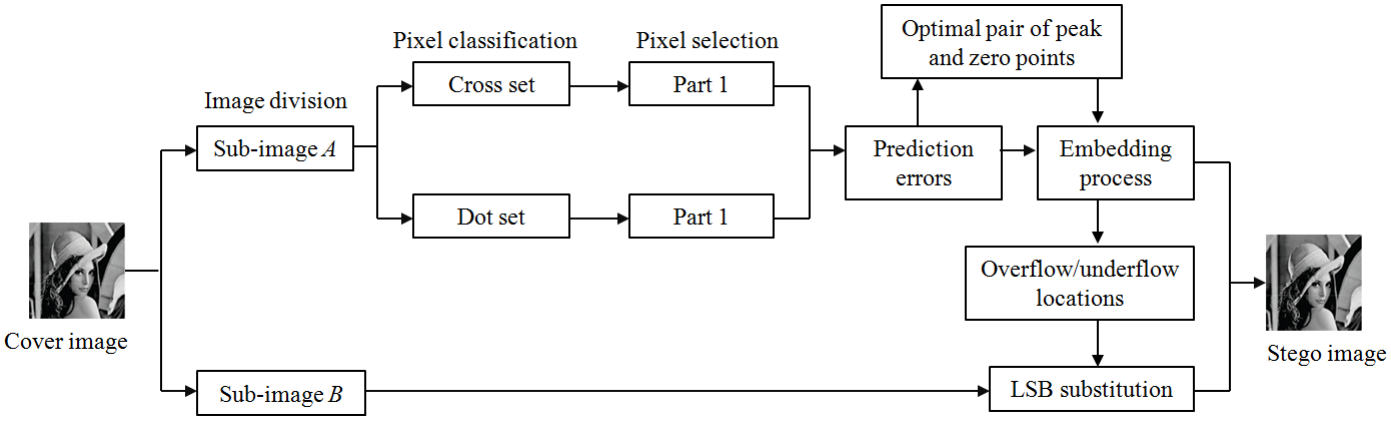

Figure 2: Flowchart of the proposed embedding process

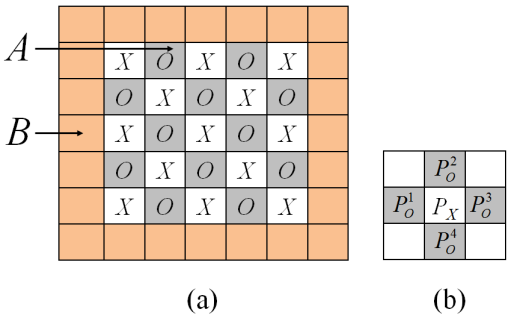

Figure 3: Division of the cover image

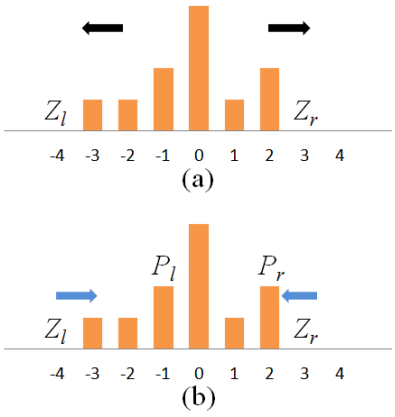

Figure 4: Division of the cover image

two steps is applied. Step 1: Search for two highest frequency points P_l and P_r on the negative and positive axes of the histogram, if $L > F(P_l)$ and $L > F(P_r)$, then select the higher frequency P as $P = maxP_l, P_r$, and the nearest zero point Z of such peak point P is selected for embedding the secret data S. After that, calculate $L = L–F(P)$, and the Step 1 is repeated for the next embedding layer if $L > F(P_l)$ and $L > F(P_r)$. Otherwise, Step 2, the optimal single-layer embedding process, is used. Step 2 that is discussed above is always applied for the final-layer embedding.

Note that all of the smooth pixels (Part 1) in both the Cross and Dot sets are chosen to conceal the secret data, and these pixels are modified by no more than one value. As a result, few pixels may cause an overflow/underflow of the pixels. Therefore, instead of using the location map as was done in [18, 24], that is time-consuming and distorts the cover image significantly since the large size of location map is also embedded into the cover image because of the reversibility reason. The proposed method only records those overflow/underflow locations into the binary sequence BS. In the proposed method, not only selecting the optimal pair of peak and zero points, to minimize the embedding distortion, but threshold TH is also taken as the smallest one such that the proposed method has the ability to embed the required capacity. Then, the sub-image B is used to contain extra information, *i.e.*, the binary sequence BS, the optimal pair (P^*, Z^*), and the threshold TH by LSB substitution. It is noted that the size of sub-image B should be contained the extra information completely. Table 1 shows that our scheme with different selected thresholds TH for single-layer embedding achieves better than previous schemes since the proposed method achieves the greater virtual quality for different images. It is obvious that our method shows the effectiveness of a combination of adaptive rhombus prediction and the pixel selection strategy.

Table 1: Performance comparison of the proposed method with different selected threshold TH for single-layer embedding

Image	Criteria	TH = 5	TH = 10	TH = 15	TH = 20	[18]	[14]	[11]	[24]
Lena	Pure EC	0.159	0.246	0.280	0.296	0.138	0.236	0.114	0.150
Lena	PSNR	57.42	54.65	52.02	51.77	52.60	48.12	53.62	52.51
Baboon	Pure EC	0.009	0.026	0.041	0.051	0.030	0.040	0.039	0.033
Baboon	PSNR	64.62	60.01	56.80	55.87	49.58	47.88	50.03	48.62
Boat	Pure EC	0.220	0.257	0.293	0.274	0.080	0.149	0.109	0.078
Boat	PSNR	56.41	54.88	52.28	53.77	52.40	47.36	52.22	53.52
Sailboat	Pure EC	0.112	0.152	0.206	0.241	0.083	0.140	0.101	0.072
Sailboat	PSNR	52.64	48.12	46.04	45.78	52.18	47.25	52.89	52.87
Peppers	Pure EC	0.131	0.230	0.254	0.268	0.080	0.151	0.100	0.075
Peppers	PSNR	57.61	52.73	53.57	53.11	53.12	47.32	53.60	53.59
Airplane	Pure EC	0.246	0.315	0.332	0.340	0.249	0.299	0.179	0.199
Airplane	PSNR	55.94	53.69	51.82	51.52	51.33	47.14	55.63	51.32

3.2 Extracting Algorithm

The extracting algorithm contains five steps. Firstly, the stego image is divided into sub-image A and sub-image B. Later on, LSB bits are extracted from the sub-image B, to determine whether pixels contained the secret data or not. The threshold TH and the optimal pair of peak and zero points are also read from LSB bits in the sub-image B. According to the embedding algorithm, after obtaining the values of stego pixels P''_X in the Cross set, the same steps are used to embed the secret data into pixels of the Dot set to generate stego pixels P''_O. Therefore, to maintain the reversibility, in the extracting algorithm, the secret data are extracted from pixels of the Dot set P''_O and the Cross set P''_X, respectively. The extracting algorithm is used for reconstructing the secret bits S and restoring to the original version of cover images as following.

Step 1 (Pixel Partition): Separate the stego image into two sub-images, *i.e.*, A and B. Then, from B, read LSBs to determine overflow/underflow locations BS, TH, and (P^*, Z^*). Partition the sub-image Ainto two sets, Cross (X) and Dot (O) sets.

Step 2 (Pixel selection): For each stego pixel P''_O in the Dot set, and $P''_O \notin X$, re-calculate its local-variance (LV) using Equation (4). Then, according to the local variance and the threshold TH, pixels P''_O are classified into Part 1 or Part 2.

- Part 1 (smooth pixels): $\{P''_O \in O : LV_O < TH$, and $P''_O \notin X\}$.
- Part 2 (complex pixels): $\{P''_O \in O : P''_O \notin Part1\}$.

Step 3 (Computation of prediction errors): Compute the predicted value P'_O of the current stego-pixel P''_O by Equation (5), and determine the corresponding stego prediction error E'_O in the Dot set as

$$E'_X = P''_O - P'_O. \tag{9}$$

Step 4 (Extracting process): Based on the extracted optimal pair (P^*, Z^*), the secret bit si is extracted by Equation (10), and Equation (11) is used to restore the prediction error.

$$s_i = \left\{ \begin{array}{ll} 0, & \text{if } E'_O = P^* \\ 1, & \text{if } E'_O = P^* + 1. \end{array} \right\} \tag{10}$$

$$E_O = \left\{ \begin{array}{ll} E'_O - 1, & \text{if } E'_O \in (P^*, Z^*] \\ E'_O, & \text{otherwise} \end{array} \right\} \tag{11}$$

Then, pixels of Part 1 in the Dot set are reconstructed as

$$P_O = P'_O + E_O. \tag{12}$$

Step 5 (Restoration of the original image): According to the values of reconstructed pixels P_O in the Dot set, same steps are used to extract the secret data from pixels of the Cross set and reconstruct the original pixels P_X in the Cross set. Then, the cover image I is restored by combining of P_X and P_O. Once the secret data S is completely extracted, it is divided into the secret message M and the bit stream LSB_B. Then, LSBs of pixels in B is replaced with LSB_B to recover the original image I. It is noted that, when these five steps are performed completely, the secret message M is extracted correctly and the original image I is restored precisely.

4 Experimental Results

In this section, all results of the proposed method are analyzed in comparison with four previous schemes [11, 14, 24, 25]. Six grayscale images with a size of 512×512 in Figure 5, were used in the experiment. It is noted that two different schemes are introduced in [11]. Their scheme 1 provided the higher EC, whereas the better image quality was obtained by their scheme 2 when the small EC was embedded. To make a fair comparison, only

the best results of each scheme were used for comparison.Figure 6shows the comparison results of our scheme and four other schemes. Here, we vary the embedding rate (ER) from 0.1 bpp to its maximum with the step size 0.1. Figure 6 shows that, for all of the six tested images, the proposed method achieved superior performance to those of four previous schemes [11, 14, 24, 25]. The proposed method yielded a very good image quality with high EC. Lena image can be taken as an example. When the embedding rate is 0.6 bpp, the proposed method still maintains the good image quality (larger than 45 dB). The performance of Wang *et al.*'s scheme [25] is superior to those of three schemes [11,14,24] when embedding the secret data of small sizes. This is because, in the scheme [25], smooth pixels were also selected based on the GA algorithm. However, our scheme still outperforms Wang *et al.*'s scheme [25]. In particular, the proposed method produced the greater virtual image quality than the scheme [25], when average gains are 2.94 dB and 2.39 dB for an EC of 10,000 bits, 20,000 bits, respectively, with single-layer embedding, as can be seen in Tables 2 and 3. Although the proposed method and two other schemes [24,25] are based on both histogram shifting and rhombus prediction techniques, however, the better performance was obtained by the proposed method than by two other schemes [24,25] in most cases. In the proposed method, the threshold TH is used to control selected pixels, which guarantees that only pixels in the smooth region are embedded into the secret bits. Moreover, the adaptive rhombus prediction technique is utilized to reduce the embedding distortion in complex regions. In addition, instead of using the pair of peak and zero points as in existing HS-based RDH schemes, our method selected the most suitable one of the peak and zero points for embedding data, which is another reason for the superior of the proposed method (see in Figure 6).

In addition, the performance obtained from the proposed method is compared with six previous schemes [6, 11, 14, 24, 25, 27] at low embedding capacity when single-layer embedding is applied. Tables 2 and 3 show the comparison results for EC of 10,000 bits and 20,000 bits, respectively. From Tables 2 and 3, it is obvious that the proposed method shows better image quality than other existing schemes. Table 4 shows that the optimal pairs and sets are used for embedding with different sizes of the secret data. It is noted that the proposed method used different pairs of peak and zero points to minimize embedding distortion when the different sizes of secret data are embedded.

5 Conclusions

In this article, a novel HS-based RDH method based on the combination of adaptive rhombus prediction algorithm and pixel selection technique is proposed. To increase the EC while guaranteeing the small distortion of stego images, the local variance value of pixels in the cover image is calculated to determine embeddable pixels. Moreover, adaptive rhombus prediction algorithm is used for calculating the prediction errors. Then, optimal information is used in the proposed embedding phase to guarantee high performance. Experimental results suggested that the performance of our proposed method is improved further in comparison with previously rhombus prediction HS-based RDH techniques in terms of the EC and the image quality.

Acknowledgments

This study was supported by the Tra Vinh University under grant 207/HD-HDKH-DHTV. The authors gratefully acknowledge the anonymous reviewers for their valuable comments.

References

[1] C. C. Chang and T. S. Nguyen, "A reversible data hiding scheme for SMVQ indices," *Informatica*, vol. 25, no. 4, pp. 523–540, 2014.

[2] C. C. Chang, T. S. Nguyen, and C. C. Lin, "A virtual primary key for reversible watermarking textual relational databases," in *Intelligent Systems and Applications*, pp. 756–769, Dec. 2014.

[3] C. C. Chang, T. S. Nguyen, and C. C. Lin, "A reversible compression code hiding using soc and SMVQ indices," *Information Sciences*, vol. 300, no. 10, pp. 85–99, 2015.

[4] W. J. Chen and W. T. Huang, "Vq indices compression and information hiding using hybrid lossless index coding," *Digital Signal Processing*, vol. 19, no. 3, pp. 433–443, 2009.

[5] G. Y. Gao, S. K. Tong, Z. H. Xia, B. Wu, L. Xu, and Z. Q. Zhao, "Reversible data hiding with automatic contrast enhancement for medical images," *Signal Processing*, vol. 178, 2021.

[6] W. He, K. Zhou, J. Cai, L. Wang, and G. Xiong, "Reversible data hiding using multi-pass pixel value ordering and prediction-error expansion," *Journal of Visual Communication and Image Representation*, vol. 49, pp. 351–360, 2017.

[7] W. Hong, T. S. Chen, and C. W. Shiu, "Reversible data hiding for high quality images using modification of prediction errors," *Journal of Systems and Software*, vol. 82, no. 11, pp. 1833–1842, 2009.

[8] Y. Hu, H. K. Lee, and J. Li, "De-based reversible data hiding with improved overflow location map," *IEEE Transactions on Circuits and Systems for Video Technology*, vol. 19, no. 2, pp. 250–260, 2009.

[9] R. Kumar and K. H. Jung, "Robust reversible data hiding scheme based on two-layer embedding strategy," *Information Sciences*, vol. 512, pp. 96–107, 2020.

[10] J. D. Lee, Y. H. Chiou, and J. M. Guo, "Reversible data hiding based on histogram modification

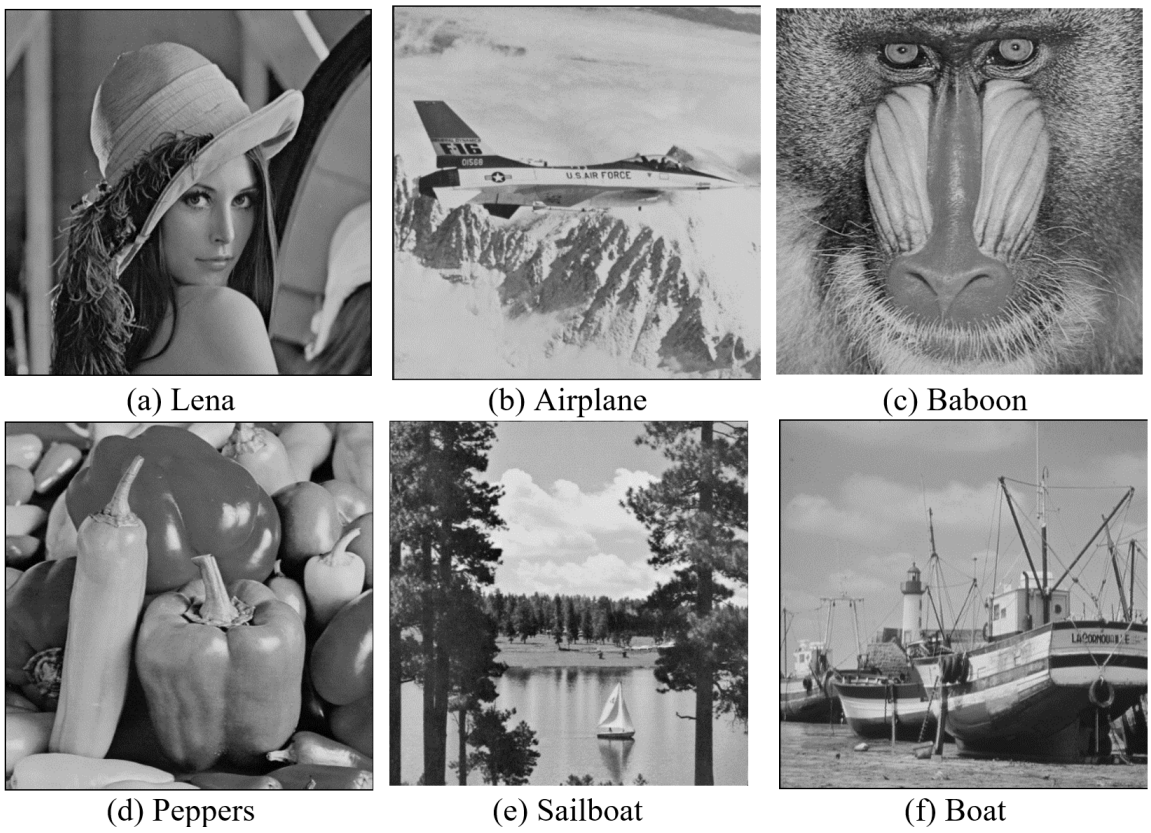

Figure 5: Six tested grayscale images sized 512x512

Table 2: Comparison of the image quality (dB) of five RDH schemes for EC of 10,000 bits with single-layer embedding

Images	**Proposed**	**Xiao [27]**	**Wang [25]**	**He [6]**	**Li [11]**	**Luo [14]**	**Wang [24]**
Lena	62.37	60.92	60.14	60.64	59.37	57.35	57.94
Airplane	63.42	63.97	61.93	63.45	62.65	57.97	59.25
Baboon	56.53	56.23	55.22	54.01	54.41	51.08	52.61
Peppers	62.40	58.76	58.04	59.29	56.89	55.23	56.64
Sailboat	61.68	59.87	57.45	59.71	58.27	55.74	57.38
Boat	61.47	58.34	57.47	58.28	57.16	54.07	56.31
Average	61.31	59.68	58.38	59.23	58.13	55.24	56.69
Gain of PSNR	-	1.63	2.94	2.08	3.19	6.07	4.62

Table 3: Comparison of the image quality (dB) of five RDH schemes for EC of 20,000 bits with single-layer embedding

Images	**Proposed**	**Xiao [27]**	**Wang [25]**	**He [6]**	**Li [11]**	**Luo [14]**	**Wang [24]**
Lena	59.64	57.32	56.81	56.81	55.93	53.85	55.87
Airplane	59.28	60.47	59.59	59.59	59.26	55.44	57.31
Peppers	58.36	54.99	55.11	55.11	53.31	52.26	53.71
Sailboat	58.47	54.58	54.53	54.53	53.19	52.17	54.58
Boat	56.31	54.13	54.07	54.07	53.05	51.19	53.36
Average	58.41	56.30	56.02	56.02	54.95	52.98	54.97
Gain of PSNR	-	2.11	2.39	2.39	3.46	5.43	3.45

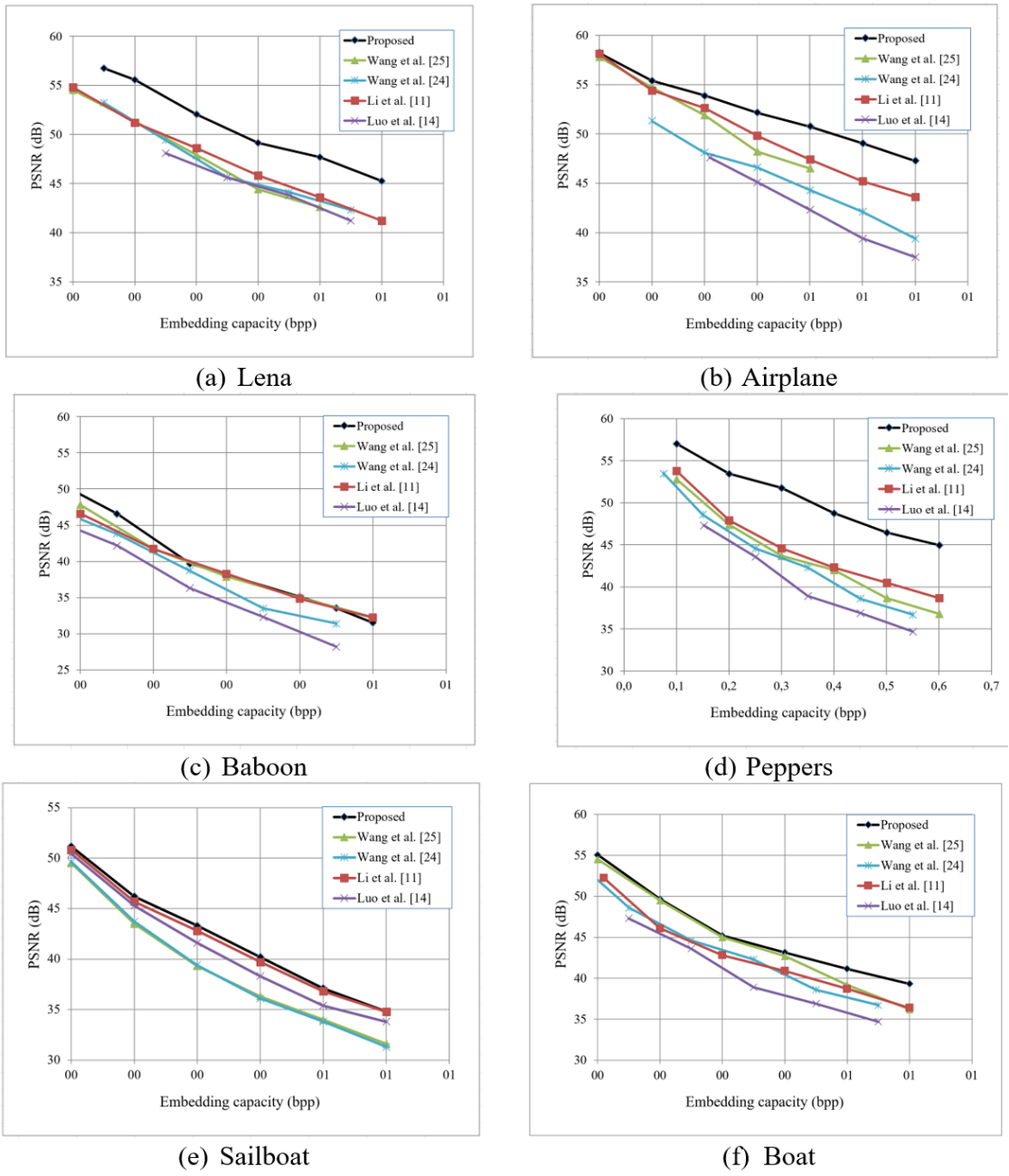

Figure 6: Performance comparison of the proposed method and four previous schemes [11, 14, 24, 25]

Table 4: Parameters used by the proposed method with the threshold TH = 5 for Lena image at low EC

ER (bpp)	Embedding set	Optimal peak and zero points	PSNR (dB)
0.035	Cross	1,20	62.87
0.035	Dot	(-1,-18)	62.31
0.09	Cross	0,20	59.12
0.09	Dot	(0,-18)	59.14
0.12	Cross	0,20	59.11
0.12	Dot	(0,-18)	57.72

of SMVQ indices," *IEEE Transactions on Information Forensics and Security*, vol. 5, no. 4, pp. 638–648, 2010.

[11] X. Li, B. Li, B. Yang, and T. Zeng, "General framework to histogram-shifting-based reversible data hiding," *IEEE Transactions on Image Processing*, vol. 22, no. 6, pp. 2181–2191, 2013.

[12] X. Li, B. Yang, and T. Zeng, "Efficient reversible watermarking based on adaptive prediction-error expansion and pixel selection," *IEEE Transactions on Image Processing*, vol. 20, no. 12, pp. 3524–3533, 2011.

[13] M. Long, Y. Zhao, X. Zhang, and F. Peng, "A separable reversible data hiding scheme for encrypted images based on tromino scrambling and adaptive pixel value ordering," *Signal Processing*, vol. 176, 2020.

[14] L. Luo, Z. Chen, M. Chen, X. Zeng, , and Z. Xiong, "Reversible image watermarking using interpolation technique," *IEEE Transactions on Information Forensics and Security*, vol. 5, no. 1, pp. 187–193, 2010.

[15] D. C. Nguyen, T. S. Nguyen, F. R. Hsu, and H. Y. Hsien, "A novel steganography scheme for video H. 264/AVC without distortion drift," *Multimedia Tools and Applications*, vol. 78, no. 12, pp. 16033–16052, 2019.

[16] Z. Ni, Y. Q. Shi, N. Ansari, and W. Su, "Reversible data hiding," *IEEE Transactions on Circuits and Systems for Video Technology*, vol. 16, no. 3, pp. 354–362, 2006.

[17] F. Peng, X. Li, and B. Yang, "Adaptive reversible data hiding scheme based on integer transform," *Signal Processing*, vol. 92, no. 1, pp. 54–62, 2012.

[18] V. Sachnev, H. J. Kim, J. Nam, S. Suresh, and Y.Q. Shi, "Reversible watermarking algorithm using sorting and prediction," *IEEE Transactions on Circuits and Systems for Video Technology*, vol. 19, no. 7, pp. 989–999, 2009.

[19] D. M. Thodi and J. J. Rodriguez, "Expansion embedding techniques for reversible watermarking," *IEEE Transactions on Image Processing*, vol. 16, pp. 721–730, 2007.

[20] J. Tian, "Reversible data hiding using a difference expansion," *IEEE Transactions on Circuits and Systems for Video Technology*, vol. 13, pp. 890–896, 2003.

[21] P. H. Vo, T. S. Nguyen, V. T. Huynh, and T. N. Do, "A novel reversible data hiding scheme with two-dimensional histogram shifting mechanism," *Multimedia Tools and Applications*, vol. 77, no. 21, pp. 28777–28797, 2018.

[22] P. H. Vo, T. S. Nguyen, V. T. Huynh, T. C. Vo, and T. N. Do, "Secure and robust watermarking scheme in frequency domain using chaotic logistic map encoding," in *Advanced Computational Methods for Knowledge Engineering*, pp. 346–357, Dec. 2019.

[23] P. H. Vo, T. S. Nguyen, V. T. Huynh, T. C. Vo, and T. N. Do, "A high-capacity invertible steganography method for stereo image," *Digital Media Steganography*, pp. 99–122, 2020.

[24] J. Wang, J. Ni, and Y. Hu, "An efficient reversible data hiding scheme using prediction and optimal side information selection," *Journal of Visual Communication and Image Representation*, vol. 25, pp. 1425–1431, 2014.

[25] J. Wang, J. Ni, X. Zhang, and Y. Q. Shi, "Rate and distortion optimization for reversible data hiding using multiple histogram shifting," *IEEE Transactions on Cybernetics*, vol. 47, no. 2, pp. 315–326, 2017.

[26] J. X. Wang and Z. M. Lu, "A path optional lossless data hiding scheme based on vq joint neighboring coding," *Information Sciences*, vol. 179, no. 19, pp. 3332–3348, 2009.

[27] M. Xiao, X. Li, Y. Wang, Y. Zhao, and R. Ni, "Reversible data hiding based on pairwise embedding and optimal expansion path," *Signal Processing*, vol. 158, pp. 210–218, 2019.

[28] J. Zhou and O. C. Au, "Determining the capacity parameters in pee-based reversible image watermarking," *IEEE Signal Processing Letters*, vol. 19, no. 5, pp. 287–290, 2012.

Biography

Thai-Son Nguyen received the M.S. and Ph.D. degrees from Feng Chia University, Taichung, Taiwan, in 2011 and 2015, respectively, all in computer science. he served as a lecturer in Tra Vinh University,Vietna, from 2006. From 2019, he was Dean of the school of Engineering and Technology, Tra Vinh University. He is currently an Associate professor. His research interests include image processing, information hiding, image recognition, information security, and artificial intelligence applications.